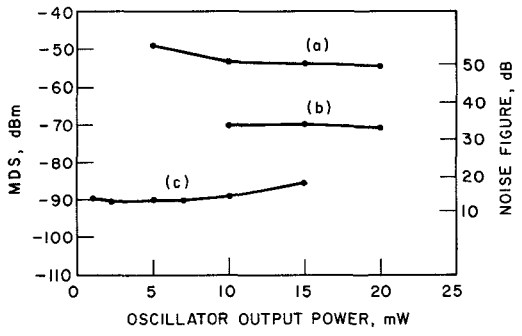

Fig. 13. MDS at different output-power levels. (a) IMPATT device. (b) Gunn device. (c) BARITT device (bandwidth = 10 MHz, IF = 30 MHz).

IV. Discussion of Results

In terms of sensitivity, the BARITT device is superior at any power level and modulation frequency. An outstanding characteristic of the device is that the sensitivity is better at lower oscillator output-power levels while the reverse is true for both the Gunn and IMPATT devices. In addition, the sensitivity of the low-voltage BARITT device is comparable or better than that of the higher voltage ones. This is an important feature and a definite advantage over the other devices. Another desirable quality of the BARITT device is its insensitivity to bias variation, as can be seen in Fig. 6. This is not true for the Gunn or IMPATT devices where a slight variation in bias leads to a rapid deterioration of sensitivity. To offset this the RF circuit has to be retuned whenever the bias is slightly changed.

It is also apparent that the BARITT device does seem to possess a $1/f$ noise component. The origin of this $1/f$ noise in BARITT devices is not well understood at this time. One hesitates to conclude that it is an inherent characteristic. If this $1/f$ noise were due to some effect of the fabrication process, then eventually it could be eliminated or reduced by more sophisticated techniques of fabrication. This would greatly enhance the sensitivity of the BARITT device at the low-modulation frequency range.

V. Conclusion

It has been shown that, using the simplified design principle given here, BARITT devices of different operating voltages and frequencies can be successfully designed. While a great deal more remains to be learned about the noise and mixing characteristics of the BARITT device, the experiments described show that the BARITT device has definite advantages in self-mixing mode applications. These are, in short, low-power consumption, high sensitivity, and ease of fabrication and operation. The BARITT device also has great potential in the higher frequency region due to the fact that low output power does not affect its sensitivity.

References

[1] W. Shockley, "Negative resistance arising from transit time in semiconductor diodes," *Bell System Tech. J.*, vol. 33, pp. 799–826, July 1954.
[2] D. J. Coleman, Jr., and S. M. Sze, "A low-noise metal–semiconductor–metal (MSM) microwave oscillator," *Bell System Tech. J.*, vol. 50, pp. 1695–1699, May/June 1971.
[3] C. P. Snapp and P. Weissglas, "On the microwave activity of punchthrough injection transit-time structure," *IEEE Trans. Electron Devices*, vol. ED-19, pp. 1109–1118, Oct. 1972.
[4] S. P. Kwok, H. Nguyen-Ba, and G. I. Haddad, "Properties and potential of BARITT devices," *IEEE Int. Solid-State Circuits Conf. Digest*, Philadelphia, PA, pp. 180–181, Feb. 1974.
[5] D. J. Coleman, Jr., "Transit-time oscillations in BARITT diodes," *J. Appl. Phys.*, vol. 43, pp. 1812–1819, April 1972.
[6] A. Sjölund, "Small-signal noise analysis of punch-through injection microwave diodes," *Solid-State Electronics*, vol. 16, pp. 559–569, May 1973.
[7] G. T. Wright, "Small-signal characteristics of semiconductor punch-through injection and transit time diodes," *Solid-State Electronics*, vol. 16, pp. 903–912, August 1973.
[8] G. I. Haddad, "Basic principles and simple design procedures of BARITT devices," EPL Memo No. 75-2-005030, Electron Physics Laboratory, The University of Michigan, Ann Arbor, June 1975.

Millimeter-Wave Receivers with Subharmonic Pump

THOMAS F. McMASTER, MARTIN V. SCHNEIDER, FELLOW, IEEE, AND WILLIAM W. SNELL, JR.

Abstract—**Hybrid integrated downconverters which are pumped at half the frequency needed in a conventional downconverter have shown a conversion loss of 3 dB at 50 GHz and 6 dB at 100 GHz with a corresponding single-sideband (SSB) receiver noise figure of 7 dB at 50 GHz and 11 dB at 100 GHz. The circuits are linearly scaled from an optimized 5-GHz model. Each downconverter consists of a stripline conductor pattern, a novel transition from waveguide to stripline, and a Schottky-barrier diode pair. The circuits can be tuned over a useful RF bandwidth of 20 GHz, and they can be readily scaled to other frequency bands.**

Manuscript received May 13, 1976; revised July 23, 1976.
The authors are with Bell Laboratories, Holmdel, NJ 07733.

I. Introduction

A NEW subharmonically pumped downconverter has shown a conversion loss and an RF bandwidth which is superior to the performance of previously reported integrated converters [1], [2] and of conventional wave-

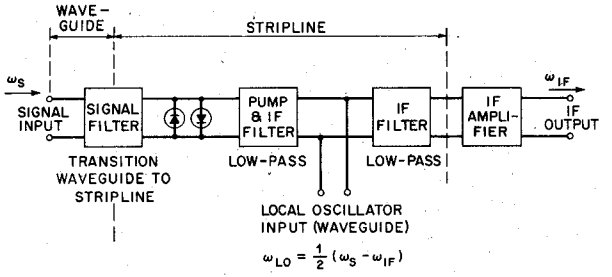

Fig. 1. Block diagram of the receiver. The signal filter is a special transition from waveguide to stripline shown in Fig. 4. The stripline circuit includes two low-pass filters and a pair of Schottky-barrier diodes. The pump is coupled to the stripline from a waveguide input as shown in Fig. 2.

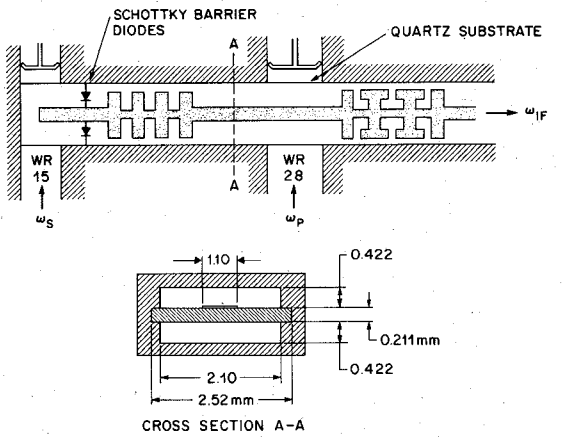

Fig. 2. Top view and cross-sectional view of the 50-GHz stripline circuit with signal and pump waveguide input ports.

guide downconverters. The converter has the following advantages.

1) The thin-film stripline medium suppresses waveguide modes at harmonics of the pump frequency.

2) The mixer can be readily tuned for single-sideband (SSB) or double-sideband operation.

3) The pump frequency is half that needed in conventional downconverters.

4) The circuit does not require a dc return path.

5) Separation of the signal and pump frequencies is readily obtained.

6) The local oscillator AM noise sidebands are suppressed [3].

Mixers have been built at 50 and 100 GHz by linearly scaling the circuit dimensions of an optimized 5-GHz model.

II. Circuit Description

A block diagram of the new circuit is shown in Fig. 1, and a detailed view of the stripline conductor pattern for the 50-GHz mixer is shown in Figs. 2 and 3. A photograph of the mixer assembly with the cover removed is shown in Fig. 4. A strip transmission line is used because the mode conversion from the hybrid TEM mode to the first-order waveguide mode (longitudinal section magnetic mode) is substantially reduced compared with the mode conversion obtained with other transmission line circuits, such as waveguide or microstrip circuits [4]. This approach helps

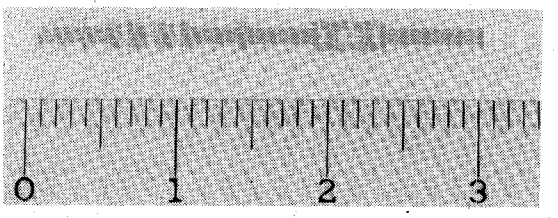

Fig. 3. Photograph of thin-film conductor pattern on quartz substrate, 50-GHz circuit. The scale is marked in centimeters.

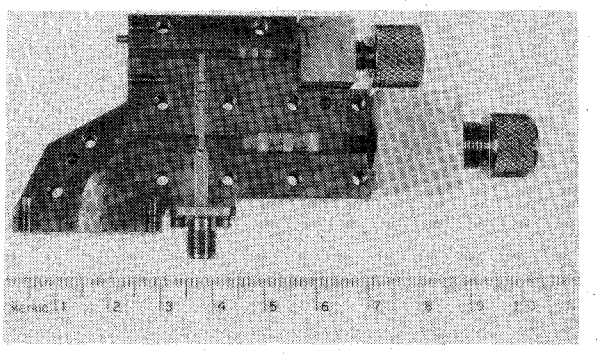

Fig. 4. Photograph of the 50-GHz downconverter. The top cover of the housing is removed to show the conductor pattern on the quartz substrate.

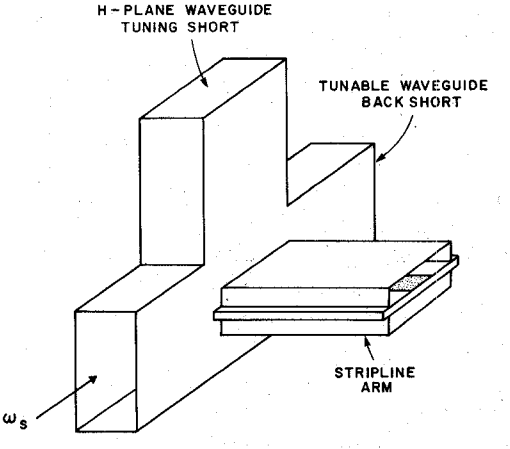

Fig. 5. Transition from signal waveguide to stripline circuit with a tunable waveguide backshort and an *H*-plane tunable short for matching the signal and rejecting the image frequency.

eliminate the generation of extraneous waveguide modes near the harmonics of the pump frequency.

The circuit consists of a signal waveguide input section, a waveguide-to-stripline transition, a stripline conductor pattern with a pair of Schottky-barrier diodes, and a transition from the pump waveguide to the stripline. The waveguide-to-stripline transition, illustrated in Fig. 5, can be tuned so that the converter can be operated either as a SSB or as a double-sideband mixer by adjusting the waveguide backshort and the *H*-plane waveguide short.

The input signal is coupled to a pair of beam lead diodes which are shunt mounted with opposite polarities in the strip transmission line. The diode pair has a current–voltage characteristic which is symmetrical with respect to the origin [1]. The diode-pair current is

$$i = I_{sat} \sinh\left[\frac{q}{nkT}(v - iR_s)\right] \tag{1}$$

where I_{sat} is the pair saturation current, q is the electron charge, and R_s is the series resistance of the device. If the pair is pumped by a sinusoidal voltage $v = V_p \cos \omega_p t$ the resulting current for $R_s = 0$ is

$$i = 2I_{sat} \sum_{m=0}^{\infty} I_{2m+1}\left(\frac{qV_p}{nkT}\right) \cos (2m + 1)\omega_p t \qquad (2)$$

where I_{2m+1} is the modified Bessel function of first kind of order $2m + 1$. The corresponding conductance is

$$\frac{di}{dv} = \frac{qI_{sat}}{nkT} I_0\left(\frac{qV_p}{nkT}\right) + 2\frac{qI_{sat}}{nkT} \sum_{m=1}^{\infty} I_{2m}\left(\frac{qV_p}{nkT}\right) \cos 2m\omega_p t. \qquad (3)$$

As expected, 1) there is no dc current flowing through the diode pair, i.e., the converter does not need a dc return path; 2) the diode-pair current contains only odd-order harmonics; and 3) the pair conductance has only even-order harmonics. Using $g(t) = di/dv$ and

$$y_j = \frac{qI_{sat}}{nkT} I_{2j}\left(\frac{qV_p}{nkT}\right), \qquad j = 0,1,2,\cdots \qquad (4)$$

one can rewrite (3) and obtain

$$g(t) = y_0 + 2y_1 \cos 2\omega_p t + 2y_2 \cos 4\omega_p t + \cdots. \qquad (5)$$

This shows that it is possible to use half-frequency pumping with an antiparallel diode pair. One concludes, furthermore, that quarter-frequency pumping is also feasible if the second term in (5) is suppressed by means of a band-reject filter at $2\omega_p$ in series with the diode pair. This solution looks attractive for submillimeter frequency conversion.

The diodes used in the subharmonically pumped circuits have a typical series resistance of 3.5 Ω, a zero bias capacitance of 0.06 pF, a reverse breakdown voltage of 7 V at a current of 10 μA, and an n-factor of 1.15. The corresponding zero bias cutoff frequency is approximately 1500 GHz.

Two low-pass filters are needed to separate the signal frequency ω_S, the pump frequency $\omega_P = (\omega_S - \omega_{IF})/2$, and the intermediate frequency (IF) ω_{IF}. The filter in the 50-GHz mixer which is adjacent to the diode pair has a cutoff frequency of 33 GHz in order to reject the signal (47–67 GHz) while transmitting the pump (22.8–32.8 GHz) and the IF (1.4 GHz). The second low-pass filter rejects the pump and transmits the IF. The thin-film chromium–gold conductor film is deposited on fused quartz substrates by evaporating 100 Å of chromium and 2.5 μm of gold. The pattern is fabricated using standard photolithographic techniques.

III. Circuit Optimization

Because of the difficulties of synthesizing an optimized millimeter-wave mixer, it was decided to build an oversized low-frequency model. This circuit was built at 5 GHz with the objective of scaling it to 50 and 100 GHz. The laws governing the scaling of electromagnetic circuits are described by Stratton [5]. In order to obtain circuits with similar characteristics at different frequencies, each with a characteristic dimension d, an RF frequency ω, a conductivity σ, permeability μ, and permittivity ε, it is necessary and sufficient that

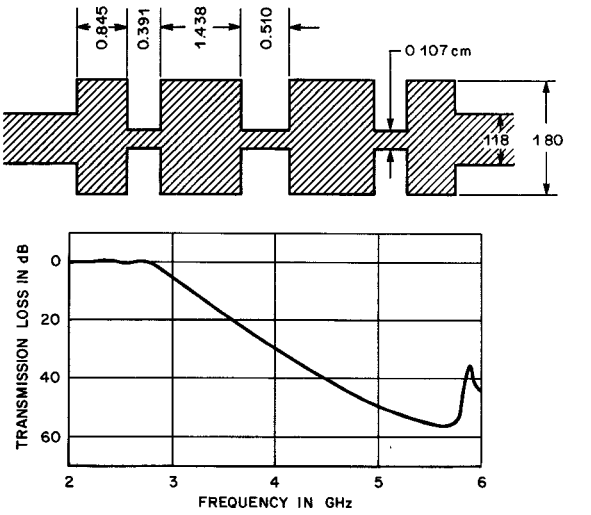

Fig. 6. Performance of stripline low-pass filter located between signal and pump waveguide. The filter is made with copper tape on a fused quartz substrate with a thickness of 2.26 mm and a width of 2.71 cm. All filter dimensions are given in centimeters.

$$\mu\varepsilon(\omega d)^2 = K_1 \qquad (6)$$

$$\mu\varepsilon\sigma\omega d^2 = K_2 \qquad (7)$$

where K_1 and K_2 are constants. It should be noted that (6) and (7) can be readily satisfied for purely passive elements such as stripline conductors. Nonlinear devices such as Schottky-barrier diodes are more difficult to scale. However, satisfactory results can be obtained if the series inductance, the zero bias capacitance, and the cutoff frequency of the diode are linearly scaled to the desired millimeter-wave frequency. In order to satisfy this requirement for the low-frequency model, we chose pill-type diodes with a high zero bias capacitance and added oversized leads to simulate the series inductance of the millimeter-wave beam-lead Schottky-barrier diodes.

The dimensions of the rectangular stripline channel with the cross section shown in Fig. 2 must be such that the first-order waveguide mode at the signal frequency is below cutoff. The cutoff frequency of this mode is given by [6]

$$f_c = \frac{c}{2a}\sqrt{1 - \frac{h(\varepsilon_r - 1)}{b\varepsilon_r}} \qquad (8)$$

where a is the width of the channel, b is the height, h is the thickness of the dielectric material, ε_r is its relative dielectric constant, and c is the vacuum velocity of light. The channel dimensions for the 5-GHz model are $a = 2.26$ cm, $b = 1.13$ cm, and the thickness of the fused quartz substrate is 0.226 cm. The relative dielectric constant of the substrate is 3.8 and the resulting cutoff frequency becomes 6.13 GHz.

The conductor patterns for the 5-GHz model were made with copper tape on quartz substrates. This technique makes it convenient to experimentally determine the exact dimensions and positions of the filter circuits. The dimensions and the electrical characteristics of the stripline filters are shown in Figs. 6 and 7. The filter between the pump and

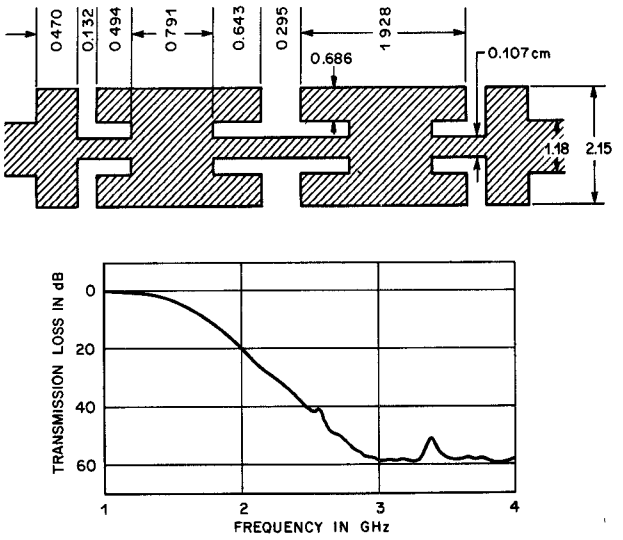

Fig. 7. Performance of stripline low-pass filter between the pump waveguide and the IF output port. The filter is made with copper tape on a fused quartz substrate with a thickness of 2.26 mm and a width of 2.71 cm. All filter dimensions are given in centimeters.

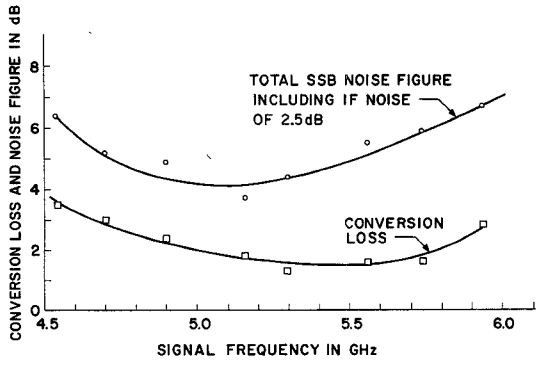

Fig. 8. Measured conversion loss and SSB noise figure for 5-GHz model. The circuit is tuned at each measured frequency for best noise figure.

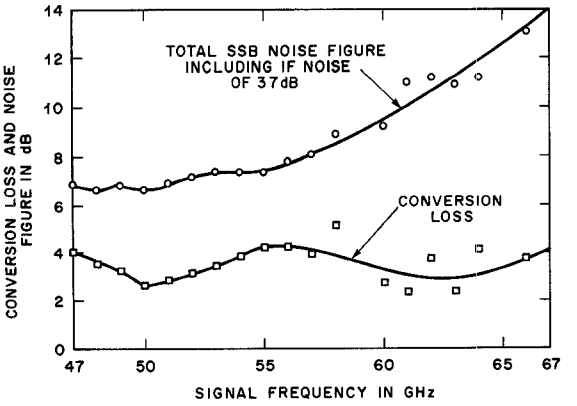

Fig. 9. Total SSB noise figure, including a 3.7-dB IF noise contribution, and conversion loss of the downconverter as a function of frequency from 47 to 67 GHz. The data points are obtained by adjusting the tunable shorts for optimum noise figure at each frequency.

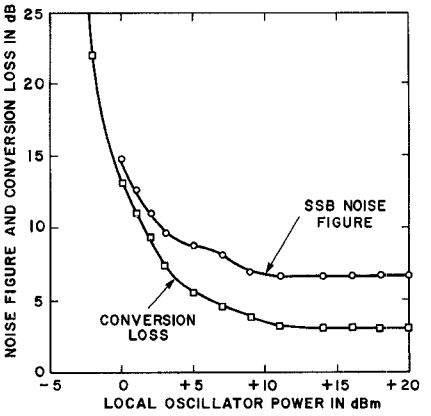

Fig. 10. Conversion loss and SSB noise figure of the downconverter at 50 GHz as a function of the pump power of the subharmonic local oscillator. The conversion loss at a pump power of +11 dBm is 2.7 dB.

signal waveguide is based on a Chebyshev design with alternate capacitive and inductive sections. The remaining filter was empirically designed to have a cutoff frequency of 1.4 GHz and a rejection of better than 40 dB at the pump frequency $\omega_p = 2.4$ GHz.

The performance of the 5-GHz model with an IF frequency of 140 MHz is shown in Fig. 8. The measured conversion loss is 1.8 dB at a frequency of 5.14 GHz. The measured SSB receiver noise figure is 3.7 dB with an IF noise figure of 2.5 dB.

A scaling factor of 10.75 was used to produce a millimeter-wave circuit at 55 GHz. The millimeter-wave mixer works satisfactorily at this frequency but its best performance is obtained at 50 GHz. This difference is mainly due to the difficulty of scaling the diode parameters.

IV. Millimeter-Wave Performance

The measured conversion loss and the SSB noise figure of the receiver, including a 3.7-dB IF noise contribution, are shown in Fig. 9. The data points are obtained by adjusting the tunable shorts for optimum noise figure at each frequency. A best conversion loss of 2.7 dB and a total SSB noise figure of 6.7 dB are obtained at 50 GHz. The conversion loss is determined by direct power measurements at 50 and 1.4 GHz. The noise measurements are made with both a calibrated waveguide noise source and by standard hot-cold load techniques. The agreement is within 0.4 dB. The mixer noise ratio is given by [7]

$$N_R = 1 + \frac{F_{SSB} - L \cdot F_{IF}}{L} \tag{9}$$

where F_{SSB} is the total SSB noise figure, F_{IF} is the IF noise figure, and L is the conversion loss of the mixer. The mixer noise ratio obtained at 50 GHz for a local oscillator pump level of +11 dBm is 1.17. The SSB noise figure and the conversion loss as a function of pump power are plotted in Fig. 10. Each point is obtained by adjusting the position of the backshort in the pump waveguide for minimum noise figure. It was found that it is not necessary to use a matched diode pair for obtaining good performance. The dc imbalance current for different diode pairs was in the range of 0.25–1.0 mA under optimum pump conditions.

Another millimeter-wave mixer was built in the 100-GHz frequency range. The measured performance is shown in

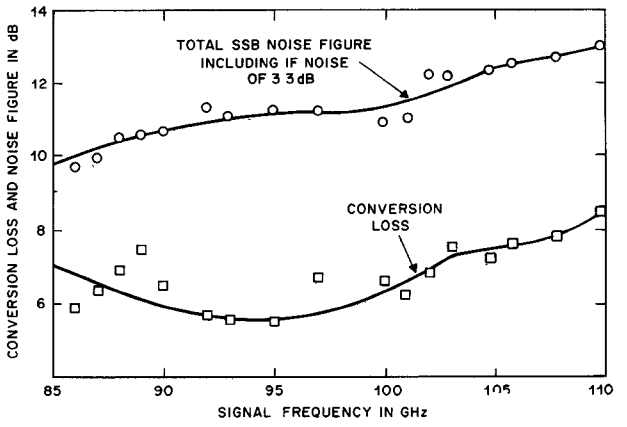

Fig. 11. Total SSB noise figure, including a 3.3-dB IF noise contribution, and conversion loss of the downconverter from 86 to 110 GHz. The data points are obtained by adjusting the tunable shorts for optimum noise figure at each frequency.

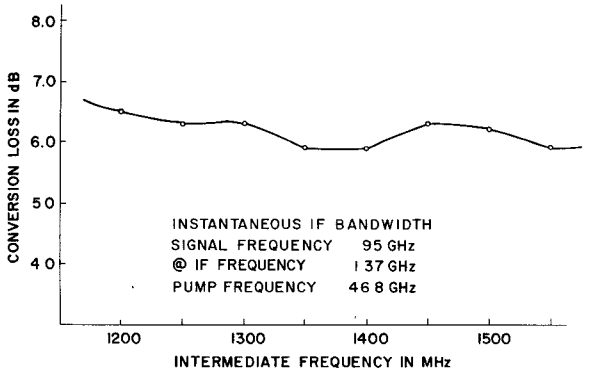

Fig. 12. Typical instantaneous IF bandwidth of the millimeter-wave mixer. The pump frequency is held constant at 46.8 GHz. The signal frequency is varied around 95 GHz to obtain the band shape.

Fig. 11. A conversion loss of 5.5 dB and a SSB receiver noise figure of 10.9 dB have been measured at 95 GHz. The noise figure measurements for this circuit were made using standard hot–cold load techniques. The measured instantaneous IF bandwidth for this mixer, tuned for optimum noise figure, is 400 MHz for a total variation of 0.5 dB as shown in Fig. 12. The circuit is thus useful as a front end in digital communication systems with modulation rates of up to 300 MBd. The mixer also exhibits excellent pump-to-signal port isolation. The pump frequency is totally suppressed since it is below cutoff in the signal waveguide. The measured output power at the signal port at the second harmonic of the pump frequency is 34 dB below the input power at the pump port. The third harmonic is suppressed by better than 28 dB.

V. Conclusions

It has been demonstrated that mixers with very low noise figures can be fabricated using a combination waveguide–stripline thin-film circuit. These mixers have shown better performance than microstrip mixers and conventional waveguide downconverters. The circuits can be readily scaled to other frequency bands.

Acknowledgment

The authors wish to thank R. F. Trambarulo, E. R. Carlson, and D. C. Redline for helpful suggestions. They also wish to thank A. C. Chipaloski for performing precision measurements.

References

[1] M. V. Schneider and W. W. Snell, Jr., "Harmonically pumped stripline down-converter," *IEEE Trans. Microwave Theory Tech.*, vol. MTT-23, pp. 271–275, March 1975.
[2] M. Cohn, J. E. Degenford, and B. A. Newman, "Harmonic mixing with antiparallel diode pair," *IEEE Trans. Microwave Theory Tech.*, vol. MTT-23, pp. 667–673, August 1975.
[3] P. S. Henry, B. S. Glance, and M. V. Schneider, "Local-oscillator noise cancellation in the subharmonically pumped down-converter," *IEEE Trans. Microwave Theory Tech.*, vol. MTT-24, pp. 254–257, May 1976.
[4] M. V. Schneider and B. S. Glance, "Suppression of waveguide modes in strip transmission lines," *Proc. IEEE*, vol. 62, p. 1184, August 1974.
[5] J. A. Stratton, *Electromagnetic Theory*. New York: McGraw-Hill, 1941, pp. 488–490.
[6] M. V. Schneider, "Millimeter-wave integrated circuits," *1973 IEEE-G-MTT International Microwave Symposium Technical Digest*, pp. 16–18, June 1973.
[7] W. W. Mumford and E. H. Scheibe, *Noise Performance Factors in Communication Systems*. Dedham, MA: Horizon House—Microwave, 1968, pp. 64–66.